ResearchGate

See discussions, stats, and author profiles for this publication at: https://www.researchgate.net/publication/233988323

31P NMR and AFM studies on the destabilization of cell and model membranes by the major bovine seminal plasma protein, PDC-109-IUBMB Life 2010

DATASET · DECEMBER 2012

READS
13

4 AUTHORS, INCLUDING:

Rajeshwer Sankhala
Thomas Jefferson University
15 PUBLICATIONS **76** CITATIONS
SEE PROFILE

Anbazhagan Veerappan
SASTRA University
44 PUBLICATIONS **482** CITATIONS
SEE PROFILE

Musti J. Swamy
University of Hyderabad
139 PUBLICATIONS **2,084** CITATIONS
SEE PROFILE

Available from: Rajeshwer Sankhala
Retrieved on: 24 January 2016

IUBMB *Life*, 62(11): 841–851, November 2010

Research Communication

^{31}P NMR and AFM Studies on the Destabilization of Cell and Model Membranes by the Major Bovine Seminal Plasma Protein, PDC-109

Rajani S. Damai*, Rajeshwer S. Sankhala*, Veerappan Anbazhagan, and Musti J. Swamy
School of Chemistry, University of Hyderabad, Hyderabad – 500 046, India

Summary

The effect of PDC-109 binding to dimyristoylphosphatidylcholine (DMPC) and dipalmitoylphosphatidylglycerol (DPPG) multilamellar vesicles (MLVs) and supported membranes was investigated by ^{31}P NMR spectroscopy and atomic force microscopy. Additionally, the effect of cholesterol on the binding of PDC-109 to phosphatidylcholine (PC) membranes was studied. Binding of PDC-109 to MLVs of DMPC and DPPG induced the formation of an isotropic signal in their ^{31}P NMR spectra, which increased with increasing protein/lipid ratio and temperature, consistent with protein-induced disruption of the MLVs and the formation of small unilamellar vesicles or micelles but not inverse hexagonal or cubic phases. Incorporation of cholesterol in the DMPC MLVs afforded a partial stabilization of the lamellar structure, consistent with previous reports of membrane stabilization by cholesterol. AFM results are consistent with the above findings and show that addition of PDC-109 leads to a complete breakdown of PC membranes. The fraction of isotropic signal in ^{31}P NMR spectra of DPPG in the presence of PDC-109 was less than that of DMPC under similar conditions, suggesting a significantly higher affinity of the protein for PC. Confocal microscopic studies showed that addition of PDC-109 to human erythrocytes results in a disruption of the plasma membrane and release of hemoglobin into the solution, which was dependent on the protein concentration and incubation time. © 2010 IUBMB
IUBMB *Life*, 62(11): 841–851, 2010

Keywords BSP-A1/A2; capacitation; cholesterol efflux; atomic force microscopy; confocal microscopy.

Abbreviations AFM, atomic force microscopy; BSP, bovine seminal plasma; CSA, chemical shift anisotropy; DMPC, dimyristoylphosphatidylcholine; DMPE, dimyristoylphosphatidylethanolamine; DMPG, dimyristoylphosphatidylglycerol; DPPC, dipalmitoylphosphatidylcholine; DPPG, dipalmitoylphosphatidylglycerol; ESR, electron spin resonance; FnII, fibronectin type-II; HPLC, high-performance liquid chromatography; Lyso-PC, lysophosphatidylcholine; MLVs, multilamellar vesicles; PC, phosphatidylcholine; ^{31}P NMR, phosphorus-31 nuclear magnetic resonance; PrC, phosphorylcholine; RBC, red blood cells; SUVs, small unilamellar vesicles; TS, transverse section; TBS-I, tris buffer saline.

INTRODUCTION

In mammalian species, seminal plasma serves as a carrier to transport ejaculated spermatozoa in the female genital tract, which ultimately leads to sperm–egg fusion and fertilization. Sperm cells undergo a series of biochemical and ultrastructural changes upon ejaculation and during their residence in the female genital tract, which are collectively referred to as capacitation [*1*]. Although sperm capacitation was discovered nearly six decades ago [*2, 3*], the molecular mechanism of this process is still not clear [*4, 5*]. The seminal plasma is a complex fluid containing a variety of low molecular weight chemical species, whereas proteins are the only high molecular weight components present in it [*6*]. Among the different mammalian species, considerable attention has been focused on the proteins from bovine seminal plasma (BSP) [*7–32*]. The BSP contains a group of four closely related acidic proteins, namely BSP-A1, BSP-A2, BSP-A3, and BSP-30-kDa protein [*7–9*]. All BSP proteins are single-chain polypeptides and display a mosaic architecture, consisting of an *N*-terminal distinctly *O*-glycosylated polypeptide extension of variable length, except BSP-A3 which is not glycosylated [*8*]. BSP-A1 and BSP-A2 have identical primary structure and differ only in glycosylation; a mixture of these two proteins is referred to as PDC-109 [*10, 11*]. It is a protein with 109 amino acid residues, and contains two tandemly repeating fibronectin type-II (FnII)[1] domains [*10–13*]. Each FnII domain contains one choline-binding site [*14*]. PDC-109 exists as a polydisperse aggregate in solution and its thermal unfolding is partially reversible [*15*]. Single-crystal X-ray diffraction studies on PDC-109 complexed with phosphorylcholine show that both the

*These authors contributed equally to this work.

Additional Supporting Information may be found in the online version of this article.

Received 14 September 2010; accepted 21 October 2010

Address correspondence to: Musti J. Swamy, School of Chemistry, University of Hyderabad, Hyderabad 500046, India. Tel: +91-40-2313-4807. Fax: +91-40-2301-2460. E-mail: mjssc@uohyd.ernet.in

ISSN 1521-6543 print/ISSN 1521-6551 online
DOI: 10.1002/iub.394

choline-binding sites are on the same face of the protein [*16*]. Very recently, it has been shown that PDC-109 exhibits chaperone-like activity against a variety of target proteins, suggesting that it could help in maintaining other proteins in its environment in their functionally active conformation even under adverse conditions [*17*].

PDC-109 is present at a concentration of 15–20 mg/mL in the seminal plasma [*18*]. On ejaculation, approximately 9.5 million PDC-109 molecules bind to each spermatozoon, which is essential for sperm to achieve fertilization capability [*19*]. This is mediated by the interaction of PDC-109 with choline phospholipids and results in their extraction together with cholesterol from the sperm plasma membrane (referred to as cholesterol efflux), which is an important step in sperm capacitation [*20–23*]. In the light of these observations, the interaction of PDC-109 with lipid membranes has been investigated by various biophysical approaches. Spin-label electron spin resonance studies by our group as well as others revealed that PDC-109 exhibits highest selectivity for the choline phospholipids, although it recognizes other phospholipids such as phosphatidylglycerol and phosphatidylserine with considerably lower specificity [*24, 25*]. Additional ESR studies have shown that cholesterol modulates the interaction of PDC-109 with lipid membranes but does not directly interact with PDC-109 [*26, 27*]. Surface plasmon resonance studies indicate that binding of PDC-109 to different phospholipid membranes containing 20% (wt/wt) cholesterol occurs by a single-step mechanism [*28*]. Several observations suggest that PDC-109 may affect the structures of the lipid membranes to which it binds. Binding of PDC-109 to dimyristoylphosphatidylcholine (DMPC) multilamellar membranes resulted in a partial solubilization of the vesicles, with the mass of the particles obtained being about 1.3×10^6 daltons, which is consistent with a particle diameter of $\sim$80 nm [*24*]. Presence of cholesterol was found to stabilize the membrane structure against PDC-109-induced disruption [*28, 29*].

Although significant work has been done on the interaction of PDC-109 with phospholipid membranes, very little is known about the phase structure of the lipids in the lipoprotein aggregates resulting from PDC-109 induced disruption of lipid membranes. In the work reported here, ^{31}P NMR spectroscopic studies have been carried out on multilamellar dispersions made up of DMPC, dipalmitoylphosphatidylglycerol (DPPG) as well as with DMPC membranes containing 40 mol% cholesterol with the objective of investigating the effect of PDC-109 binding on the structure of the lipid membranes. For each lipid system, the effects of protein/lipid ratio and temperature have been investigated. The results obtained indicate that binding of PDC-109 induces the disruption of lamellar structure, leading to the formation of structures with high curvature, such as small unilamellar vesicles (SUVs) or micelles. The effect was more significant on DMPC membranes, and considerably weaker with DPPG membranes and cholesterol was found to stabilize the bilayer structure. Atomic force microscopic studies yielded results that are in good agreement with the ^{31}P NMR findings. In another set of experiments, the effect of PDC-109 binding on erythrocyte membranes was investigated by confocal microscopy as well as spectrophotometric assays. Interaction of PDC-109 with erythrocytes results in a disruption of their plasma membrane, evidenced by the release of hemoglobin from the cell into the solution. Overall, the results of the studies reported here present a clear and direct view about the action of PDC-109 on membranes made up of different phospholipids, which are consistent with the earlier observations that this protein disrupts membrane integrity [*14, 24, 25, 28, 29*]. These observations are of considerable interest in view of the crucial role played by the interaction of PDC-109 with sperm plasma membranes in sperm capacitation.

MATERIALS AND METHODS

Materials

Choline chloride (Ca^{2+} salt), tris(hydroxymethyl)-aminomethane (Tris base), acrylamide, bis-acrylamide, and TEMED were obtained from Sigma (St. Louis, MO). Sephadex G-50 (superfine) and DEAE Sephadex A-25 were purchased from Pharmacia (Uppsala, Sweden). DMPC, dipalmitoylphosphatidylcholine (DPPC), DPPG, dimyristoylphosphatidylethanolamine (DMPE), egg yolk lysophosphatidylcholine and cholesterol were products of Avanti Polar Lipids (Alabaster, AL). Sodium chloride, dichloromethane, EDTA, and sodium azide were obtained from local suppliers and were of the highest purity available.

Purification of PDC-109

PDC-109 was purified from the seminal plasma of healthy and reproductively active Ongole bulls by gel filtration on Sephadex G-50 followed by affinity chromatography on DEAE Sephadex A-25 in buffer containing 1 M NaCl [*12*] and eluted with 100-mM choline chloride [*24*], and its purity was assessed by SDS-PAGE on 10% or 12% gels [*33*]. The purified protein was dialyzed extensively against 50 mM Tris-HCl buffer, pH 7.4, containing 0.15 M NaCl, 5 mM EDTA, and 0.025% sodium azide (TBS-I) to remove the choline chloride used for elution. Concentration of PDC-109 was estimated from its extinction coefficient of 2.5 for 1 mg/mL concentration at 280 nm for 1.0-cm path length [*12*].

Confocal Microscopy

The effect of PDC-109 binding to the plasma membrane on the shape and integrity of erythrocytes was investigated by confocal microscopy. Imaging was done in the transmission mode using a Leica TCS SP2 confocal microscope (Heidelberg, Germany). Human erythrocytes (0.04%) in TBS-I buffer were used for control experiments, whereas, to monitor the interaction of PDC-109 with erythrocyte membranes, a 0.04% suspension of erythrocytes was incubated with different concentrations of PDC-109 (0.25 and 0.5 mg/mL) for an hour before imaging. Erythrocyte suspensions were directly spotted on a clean glass slide and then transferred to confocal stage for imaging.

Absorption Spectroscopy

The ability of PDC-109 to disrupt the plasma membrane of human erythrocytes was investigated by monitoring the release of hemoglobin. Assay mixture contained 200 μL of 4% RBC

suspension in TBS-I buffer, to which different amounts of PDC-109 (10–500 μg) were added, and the final volume was adjusted to 1.0 mL with TBS-I. The mixture was then incubated for 1 h at room temperature. In another experiment, 300 μg of PDC-109 was added to 0.8% RBC suspension in different vials, the volume of the suspension was adjusted to 1 mL, and then the sample was incubated for different time intervals (15–300 min). In both experiments, after incubation, the samples were centrifuged at 3,000 rpm for 5 min, the supernatant was collected and its optical density at 415 nm (which corresponds to the absorption of the haem moiety of hemoglobin) was monitored using a Shimadzu UV-3101PC UV–Vis-NIR double-beam spectrophotometer.

^{31}P NMR Spectroscopy

Samples for NMR spectroscopy were prepared by dissolving ~20–30 mg of the appropriate lipid or a mixture of the lipid and cholesterol in dichloromethane in glass tubes to give the desired final composition. The mixture was dried under a stream of nitrogen gas followed by vacuum desiccation for a minimum of 3 h. The lipid film obtained was hydrated with TBS-I (for lipid samples) or with an appropriate volume of a solution of PDC-109 in TBS-I (for lipid/protein recombinants) to give the desired lipid–protein ratio. Lipid dispersions, thus obtained, were warmed to ~50 °C in a water bath and were mildly vortexed and then subjected to eight freeze-thaw cycles to get a homogenous suspension. The lipid suspension (or lipid/protein complex), thus obtained, was transferred to a 5-mm NMR tube and centrifuged. Excess supernatant was removed, and the sample was subjected to NMR spectroscopy. ^{31}P NMR spectra were recorded at different temperatures (10–50 °C) on a Bruker Avance 400 NMR spectrometer using the zgpg30 pulse program provided by Bruker with ^{1}H decoupling with a decoupling power of 14 db. The $\pi/2$ pulse width used was 9.5 μs for ^{31}P, and the recycle delay was 1 sec. About 2,048 to 4,096 scans were accumulated for each spectrum, and the free induction decay was processed using a line broadening of 100 Hz to improve signal/noise ratio. Temperature was regulated by a thermostatted air-flow system. The spectral width was set to 400 ppm.

Atomic Force Microscopy

Supported membranes of DPPC, DMPC, and DMPG were prepared in the following manner. About 0.2 mg of the lipid was taken in a glass test tube and dissolved in about 200 μL of dichloromethane or dichloromethane/methanol mixture. The solvent was dried under a stream of nitrogen gas followed by vacuum desiccation for a minimum of 3 h. The lipid film, thus obtained, was hydrated with 1 mL of TBS-I buffer and subjected to bath sonication for 30 min. Sonicated vesicles were deposited gently on freshly cleaved mica sheets (1×1 cm^2) and kept for 30–40 min. Samples were then rinsed with HPLC grade water, dried, and transferred to the AFM stage for imaging. Experiments with DPPC membranes and studies on the interaction of PDC-109 with them were carried out in liquid cell where DPPC membrane, supported on mica, were fixed in liquid cell, and then 1 mL of TBS-I buffer was added. The cell was kept at room temperature for ~20 min to allow the membrane to attain complete hydration and then imaging was performed in contact mode by using silicon nitride cantilevers (0.6 N/m spring constant). To monitor membrane and PDC-109 interaction, about 1.5 mg of PDC-109 in TBS-I buffer was added to the same liquid cell (having membrane) and imaging was performed at different time intervals.

Experiments to investigate the interaction of PDC-109 with membranes made up of DMPC, DMPG, or DPPC/cholesterol (3:2; mol/mol) were carried out in air. Here, PDC-109 (0.5 mg/mL) was added to the sonicated lipid vesicles, before their deposition on mica and imaging was performed in semicontact mode by using NSG10 cantilevers with Au reflective coating and a nominal spring constant of 11.8 N/m. All the experiments were carried out on a SOLVER PRO-M atomic force microscope (NT-MDT, Moscow, Russia), equipped with a 3/10 μm bottom scanner and operating with a NTEGRA controller. Force was kept at the lowest possible value by continuously adjusting the setpoint and feedback gain during imaging.

RESULTS AND DISCUSSION

Binding of PDC-109 to spermatozoa results in a membrane reorganization which is a necessary event before the sperm can undergo acrosome reaction and finally fertilize the egg. Hence, considerable attention has been focused on investigating the interaction of this protein with sperm plasma membranes and model membranes [*14*]. In the present study, the interaction of PDC-109 with model membranes containing DMPC, DPPC, DMPG, and DPPG as well as with human erythrocytes was investigated by using ^{31}P NMR spectroscopy, AFM and confocal microscopy. The results obtained have been discussed below.

Confocal Microscopic and Spectrophotometric Studies on the Destabilization of Erythrocyte Plasma Membrane by PDC-109

Morphological changes in intact human erythrocytes induced by the binding of PDC-109 were monitored by confocal microscopy. The outer leaflet of the erythrocyte membranes is rich in choline phospholipids and hence provides an excellent model system to investigate the interaction of PDC-109 with cell membranes. As shown in Fig. 1A, intact human erythrocytes are 5–6 μm in size (diameter) and show a well-defined morphology, whereas erythrocytes that were incubated with 0.25 mg/mL PDC-109 for 1 h show a distorted morphology (Fig. 1B). Interestingly, incubation of erythrocytes with higher concentrations of PDC-109 (≥0.5 mg/mL) resulted in their fragmentation (Fig. 1C). PDC-109-induced disruption of erythrocytes was further investigated by monitoring the release of hemoglobin, as described below.

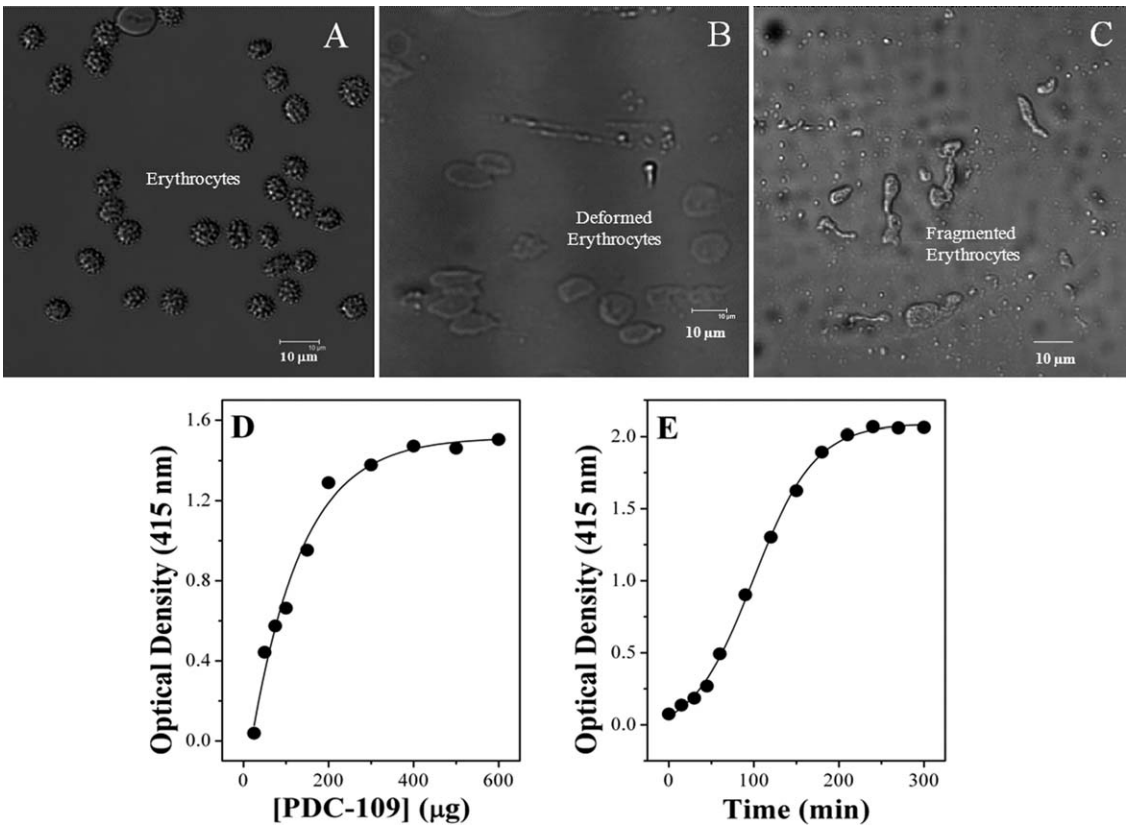

Figure 1. Effect of PDC-109 on human erythrocyte membrane. Confocal image of (A) human erythrocytes in TBS-1 buffer, (B) in the presence of 0.25 mg/mL of PDC-109 at room temperature and (C) after incubating with 0.5 mg/mL PDC-109 at room temperature. (D) Erythrocyte membrane lysis assay with increasing concentration of PDC-109. (E) Kinetics of erythrocyte membrane lysis with respect to time at a fixed concentration of PDC-109. See text for details.

Lysis of human erythrocytes resulting from the binding of PDC-109 was monitored by absorption spectroscopy. Addition of PDC-109 to the erythrocyte suspension resulted in a disruption of the erythrocyte plasma membrane, resulting in a release of hemoglobin into the solution. The content of hemoglobin increased with the increasing concentration of PDC-109, reached a maximum at about 300 μg/mL concentration of PDC-109 and then leveled off (Fig. 1D). To investigate this process further, kinetics of the release of hemoglobin from erythrocyte suspension was studied. In these experiments, erythrocyte suspensions were incubated with PDC-109 (300 μg/mL final concentration) for different time periods (15–300 min) and then centrifuged. Release of hemoglobin due to lysis was assessed by measuring the absorption as 415 nm. The results obtained revealed that release of hemoglobin into the solution increased with increasing incubation time and reached a saturation point at about 210 min (Fig. 1E). The above studies, thus demonstrate that PDC-109 can destabilize the cell membrane in a concentration- and time-dependent manner. This is of significant interest as under in vivo conditions PDC-109 interacts with sperm plasma membranes and facilitates the capacitation of spermatozoa, which is an obligatory step for successful fertilization. Studies on the interaction of PDC-109 with bovine ovarian cells also yielded essentially similar results (See supporting Information Figs. S1A and S1B).

Effect of PDC-109 on the Phase Structure of Model Membranes Studied by ^{31}P NMR Spectroscopy

Effect of PDC-109 on the phase structure of multilamellar vesicles (MLVs) made up of DMPC, DPPG, or DMPC/cholesterol (3:2; mol/mol) mixture has been investigated by ^{31}P NMR spectroscopy. All these three lipid systems yielded broad, axially anisotropic ^{31}P NMR spectra with a high-field peak and low-field shoulder, characteristic of lamellar (bilayer) membranes, both below and above the gel–liquid-crystalline phase transition temperature [*34*]. Addition of PDC-109 to DMPC MLVs led to the formation of an isotropic signal in addition to the lamellar pattern in the ^{31}P NMR spectrum, which is consistent with the disruption of the multilamellar structures by the protein and the formation of smaller aggregates [*24*]. The isotropic signal indicates that the smaller aggregates formed on

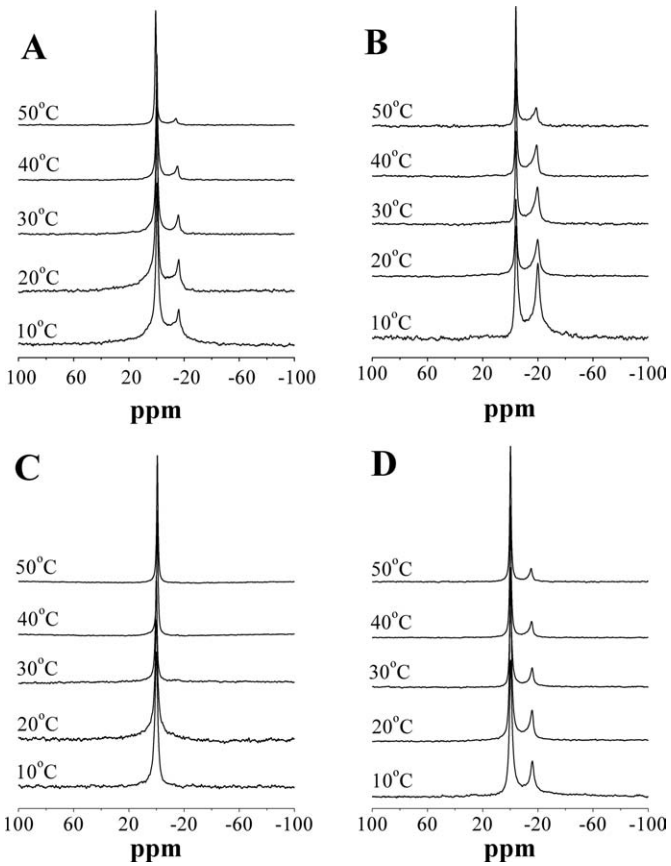

Figure 2. Interaction of DMPC model membranes with PDC-109 by ^{31}P NMR spectroscopy. ^{31}P NMR spectra of (A) DMPC in presence of PDC-109 at a lipid/protein ratio of 1:1, (B) DMPC containing 40 mol% of cholesterol in presence of PDC-109 at a lipid/protein ratio of 1:1, (C) DMPC at a protein/lipid ration of 1:1.5, (D) DMPC containing 40 mol% of cholesterol at a protein/lipid ratio of 1:1.5. All experiments were carried out at different temperatures (10 °C to 50 °C).

binding of PDC-109 to the phospholipid membranes are highly curved. Therefore, formation of structures of high curvature appears to be an integral part of the PDC-109-induced destabilization of phospholipid membranes. The results presented below clearly show that this applies not only to phosphatidylcholine (PC) membranes but also to phosphatidylglycerol membranes. The relative intensity of the isotropic signal increased with temperature, whereas the lamellar signal experienced a corresponding decrease in intensity (Figs. 2A and 2C). ^{31}P NMR spectra of DMPC/PDC-109 mixture at the ratio of 1:1 (wt/wt), both in the presence and absence of 40 mol% cholesterol, are shown in Figs. 2A and 2B. From these figures, it is seen that intensity of the isotropic signal is relatively less with DMPC membranes containing 40 mol% cholesterol (Fig. 2B). Further increase in protein/DMPC ratio resulted in an increase in the intensity of the isotropic signal. At a protein/lipid ratio of 1.5:1 (wt/wt), only isotropic signal was observed for the DMPC/PDC-109 mixture (Fig. 2C), whereas both lamellar and isotropic components were observed with samples containing 40 mol% cholesterol (Fig. 2D). For the DMPC/PDC-109 mixture, this corresponds to ~12–13 lipids per protein molecule, which is in very good agreement with the stoichiometry of ~11–13 motionally restricted lipids per PDC-109 protomer estimated by ESR spectroscopy [*24, 35*] and with the stoichiometry of 12 PC molecules to PDC-109 protomer, estimated by fluorescence measurements for maximal binding [29]. For each of the above samples, spectra were also recorded at different temperatures between 10 °C and 50 °C and in all the cases, fraction of the isotropic signal appears, to increase with increase in temperature (Fig. 2). However, in both the cases, some lamellar structure remains in the presence of cholesterol, even at higher temperatures. Even when the protein/lipid ratio was further increased to 2:1 (wt/wt), the ^{31}P NMR spectrum corresponding to the sample containing 40 mol% cholesterol contained both lamellar and isotropic components up to 40 °C, although it became nearly completely isotropic at 50 °C (Supporting Information Fig. S2).

The fractions of the lamellar and isotropic components for DMPC and DMPC containing 40 mol% cholesterol, with different lipid/protein ratios as a function of temperature are shown in Fig. 3. It is clear from this figure that for membranes made up of only DMPC, at a fixed protein/lipid ratio the fraction of isotropic component increases with increment in temperature. The fraction of isotropic component at 50 °C is approximately double that estimated at 10 °C up to a protein/lipid ratio of 1:1 (Fig. 3A, ◇ and △), whereas only isotropic component exists at higher protein/lipid ratios (Fig 3A, ▽ and □). The fraction of the isotropic signal for DMPC containing cholesterol is considerably less than that of the pure DMPC membranes, at all protein/lipid ratios and lamellar structural components can be seen even at higher protein/lipid ratios (Fig 3B, ▼ and □). These observations suggest that increasing the concentration of PDC-109 as well as sample temperature result in an increased disruption of the membrane as evidenced by the relatively higher fraction of the isotropic ^{31}P NMR signal under such conditions. As the relative fraction of the lamellar signal was found to be considerably higher in the presence of cholesterol, these studies also clearly demonstrate that cholesterol stabilizes the lamellar structure of PC membranes. This is also consistent with the previous observations which reported that cholesterol stabilizes the lamellar structure of phospholipid membranes against PDC-109-induced disruption [*14, 28, 29*].

Similar experiments were carried out with DPPG membranes at different lipid/protein ratios (Fig. 4). Addition of PDC-109 to DPPG at a lipid/protein ratio of 1:0.5 (wt/wt) resulted in only minor changes in the lamellar structure at 10 °C, with a very small isotropic peak sitting on the lamellar pattern; however, as the temperature is increased from 10 °C to 50 °C, intensity of the isotropic signal increased and the spectral intensity corresponding to the lamellar structure decreased (Fig. 4A). Further increase in protein concentration resulted in an increase in the

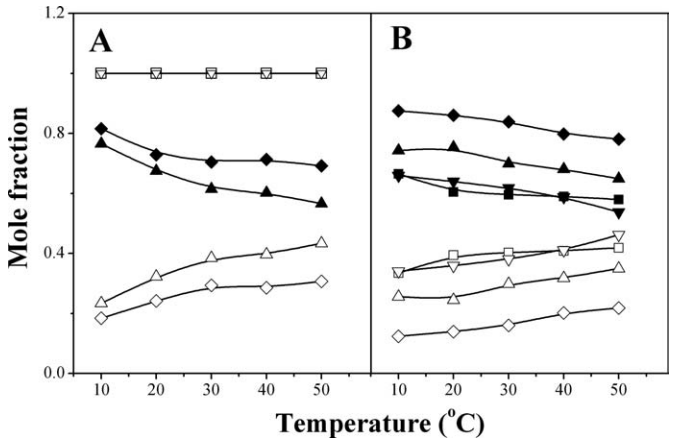

Figure 3. Variation in the fraction of the lamellar and isotropic signals in the ^{31}P NMR spectra of DMPC/PDC-109 mixtures in the absence (A) and presence (B) of cholesterol. The lipid/protein (w/w) ratios for different samples are: 1:0.5 (◆, ◇); 1:1 (▲, △); 1:1.5 (▼, ▽) and 1:2 (■, □). Closed symbols correspond to lamellar signal and open symbols correspond to isotropic signal.

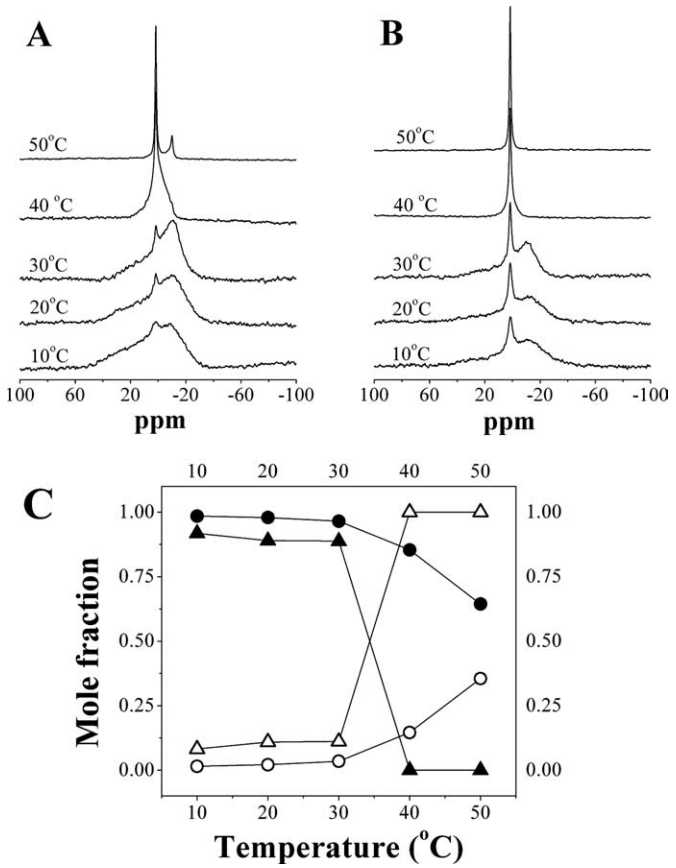

Figure 4. Interaction of DPPG model membranes with PDC-109 studied by ^{31}P NMR spectroscopy. ^{31}P NMR spectra of DPPG in presence of PDC-109 at lipid/protein ratio of 1:0.5 (A) and 1:1 (B). (C) Variation in the fraction of the lamellar and isotropic signals in the ^{31}P NMR spectra of DPPG/PDC-109 mixtures. The lipid/protein (w/w) ratios for different samples are: 1:0.5 (●, ○) and 1:1 (▲, △). Closed symbols correspond to lamellar signal and open symbols correspond to isotropic signal.

relative proportion of the isotropic signal, whose intensity increased with increase in temperature and for a lipid/protein ratio of 1:1 (wt/wt), the anisotropic signal corresponding to the lamellar phase completely disappeared at 40 °C (Fig. 4B). Temperature dependence of the relative distribution of the lamellar and isotropic signals at different DPPG/protein ratios is shown in Fig. 4C. From this figure, it can be seen that the extent of lamellar signal at different lipid/protein ratios is higher for DPPG than DMPC. Interaction of PDC-109 was also studied with DMPE membranes but no significant change was observed in ^{31}P NMR spectra of the lipid, consistent with the very weak affinity of this protein toward DMPE [*24, 28*].

The chemical shift anisotropy (CSA) values corresponding to the lamellar patterns in the ^{31}P NMR spectra of the samples made up of DMPC, DMPC/cholesterol, and DPPG containing different amounts PDC-109 are listed in Supporting Information Tables S1, S2, and S3, respectively. For the samples containing DMPC or DMPC/cholesterol (3:2; mol/mol), the CSA values are all in the range of −39 ppm and −58.1 ppm and are consistent with the lamellar structure in the gel or liquid-crystalline phase. The only exception is the spectrum recorded at 10 °C for the DMPC/PDC-109 (1:0.5; wt/wt) sample, which had a CSA value of −74.9 ppm, indicating that this sample may have some crystalline component at this low temperature. For samples containing DPPG and PDC-109 (1:0.5; wt/wt), the CSA was found to be about 60 ppm in the gel phase at 10 °C, which decreased to −47.7 ppm at 30 °C (also in the gel phase). The CSA, however, decreased significantly to −26.3 ppm at 40 °C, which is near the gel–liquid-crystalline phase transition. The CSA decreased further to −19.2 ppm at 50 °C in the liquid-crystalline phase. For the DPPG/PDC-109 sample with a L/P weight ratio of 1:1, the lamellar components in the spectra in the gel-phase region exhibited values in the range of −50 ppm to −62 ppm in the temperature range of 10–30 °C, whereas at 40 °C and above only an isotropic component was seen. The CSA values for all the samples were found to decrease with increasing temperature and are consistent with increased mobility of the lipid molecules at higher temperatures, which indicates increased disruption of the membranes at higher temperatures.

Differential scanning calorimetric studies by Gasset et al. [*29*] indicated that binding of PDC-109 to DMPC MLVs prevented the gel–liquid phase transition of the lipid. However, the effect of PDC-109 binding on the polymorphic phase structure (*i.e.*, whether the lipids adopt lamellar, inverse hexagonal, cubic, micellar, etc.), has not been investigated so far. In the present study, we have addressed this aspect using ^{31}P NMR spectroscopy. In the ^{31}P NMR spectroscopic results presented

above, formation of an isotropic signal in the presence of PDC-109 is consistent with the disruption of the DMPC MLVs and the formation of smaller aggregates. The isotropic signal further indicates the absence of hexagonal structures and suggests that the aggregates are structures with high curvature. Micelles, SUVs, and cubic phases can yield isotropic ^{31}P NMR spectra. Among these three types of aggregates, cubic structures are known to be highly viscous and visual inspection of the samples on incubation with PDC-109 at different lipid/protein ratios indicated that the samples do not exhibit high viscosity. Therefore, the formation of cubic phases on binding of PDC-109 to the different lipid systems investigated here can be excluded. However, the current ^{31}P NMR data cannot distinguish between SUVs and micelles. Addition of cholesterol at 40 mol% to DMPC led to a partial stabilization of the lamellar phase in that the fraction of the isotropic signal was less in the presence of cholesterol for the same PDC-109/DMPC ratio. These results are in agreement with the observations of Gasset et al. [*29*], who reported that the presence of cholesterol inhibited the disruption of DOPC vesicles induced by PDC-109 in a concentration-dependent manner.

AFM Studies on the Destabilization of Model Membranes by PDC-109 Binding

Supporting evidence for the conclusions drawn from the ^{31}P NMR spectroscopic studies discussed above was obtained from atomic force microscopy, which is a powerful method to study the interaction of proteins with supported membranes [*36, 37*]. Here, we have studied the effect of PDC-109 binding on the morphology of supported membranes made up of DMPC, DPPC, DMPG, and DPPC containing 40 mol% cholesterol. Upon deposition on mica, sonicated vesicles of DPPC, DMPC, and DMPG yielded well-ordered supported membranes (bilayers or multilayers) (Fig. 5, panels A, G, and I). To investigate the effect of PDC-109 binding on the structural integrity of the supported membranes, experiments were carried out both in the liquid cell and in air. Figure 5A shows the AFM image of a DPPC membrane supported on mica, obtained in a liquid cell at 25 °C, where the phospholipid is in the gel-phase. Panels A, B, and C of Fig. 5 present a typical time sequence of DPPC monolayer degradation due to removal of the phospholipid by PDC-109, whereas panels D, E, and F show the height profiles, corresponding to the white bars in panels A, B, and C, respectively. The measured height of the lipid film was found to be 6.0 ± 0.3 nm, which is in agreement with the thickness of 6.15 ± 0.93 nm reported for hydrated DPPC bilayer in the gel phase [*37*]. Incubation of the supported DPPC membrane for 10 min after the addition of PDC-109 resulted in a partial degradation of the phospholipid bilayer (Fig. 5B), whereas incubation for about 30 min led to a significant disintegration of the membrane structure (Fig. 5C). These observations support the above confocal microscopic and ^{31}P NMR findings that PDC-109 destabilizes cell and model membranes in a concentration dependent manner. Further, they demonstrate that the destabilization is also dependent on the incubation time.

Sonicated vesicles of DMPC and DMPG, which were preincubated with PDC-109, failed to form intact membrane layers. After incubation with PDC-109, no significant membranous structure of DMPC could be observed by AFM (Fig. 5H). Instead, small, nearly spherical particles, which most likely correspond to lipoprotein aggregates, were observed. The average diameter of these particles was measured to be 89 ± 7 nm, which correlates very well with the diameter of efflux particles (>80 nm) released from fibroblasts on incubation with PDC-109 [*38*]. Interestingly, electron microscopic studies by Gasset et al. [*29*] indicated that incubation of DOPC large unilamellar vesicles with PDC-109 led to the formation of particles of 10–40 nm in size. Although the exact reason for the difference in the particle size observed in the two studies is not clear, it is possible that it may be due, at least in part, to the use of the saturated phospholipid DMPC in the present study and the unsaturated DOPC by Gasset et al. [*29*]. Binding of PDC-109 to DMPG model membranes could not induce complete disintegration of the membrane, but yielded fragmented membrane layers and small membrane fragments (Fig 5J), which is consistent with the relatively lower affinity of PDC-109 for DMPG as compared with the choline-containing phospholipids [*28*].

Effect of Cholesterol

The ^{31}P NMR studies presented above have provided supporting evidence for the earlier observations that presence of cholesterol at high-mol fractions provides a significant stabilization to the lamellar structure of PC membranes [*14, 24, 28, 29*]. To investigate this further, we have carried out AFM studies on membranes made up of DPPC/cholesterol (3:2; mol/mol). Figure 6A shows that in the absence of PDC-109 intact multilayer structures are formed by this lipid mixture. Height profiles of these multilayers at two regions marked transverse section 1 (TS-1) and transverse section 2 (TS-2) are shown in Figs. 6B and 6C, respectively. Although the height profile of TS-1 shown in 6B corresponds to several layers as can be judged from the appearance of the image as well as the overall height measured (ca. 50–55 nm), the height of individual layers is not clearly discernible. On the other hand, the height profile of TS-2, shown in Fig. 6C displays a zigzag pattern and each vertical edge of the pattern, measuring about 5.0–5.5 nm most likely corresponds to the height of the bilayer as this value is comparable to the thickness of the DPPC bilayer (4.55 nm), determined by X-ray diffraction measurements [*39*]. Addition of PDC-109 to the DPPC/cholesterol multilayers results in a significant break down of the membranous structures. However, unlike in the case of membranes containing only DPPC (Fig. 6D), membrane fragments of moderate size are observed in some regions (Fig. 6E), suggesting that presence of cholesterol afforded a partial stabilization of lipid membranes, which

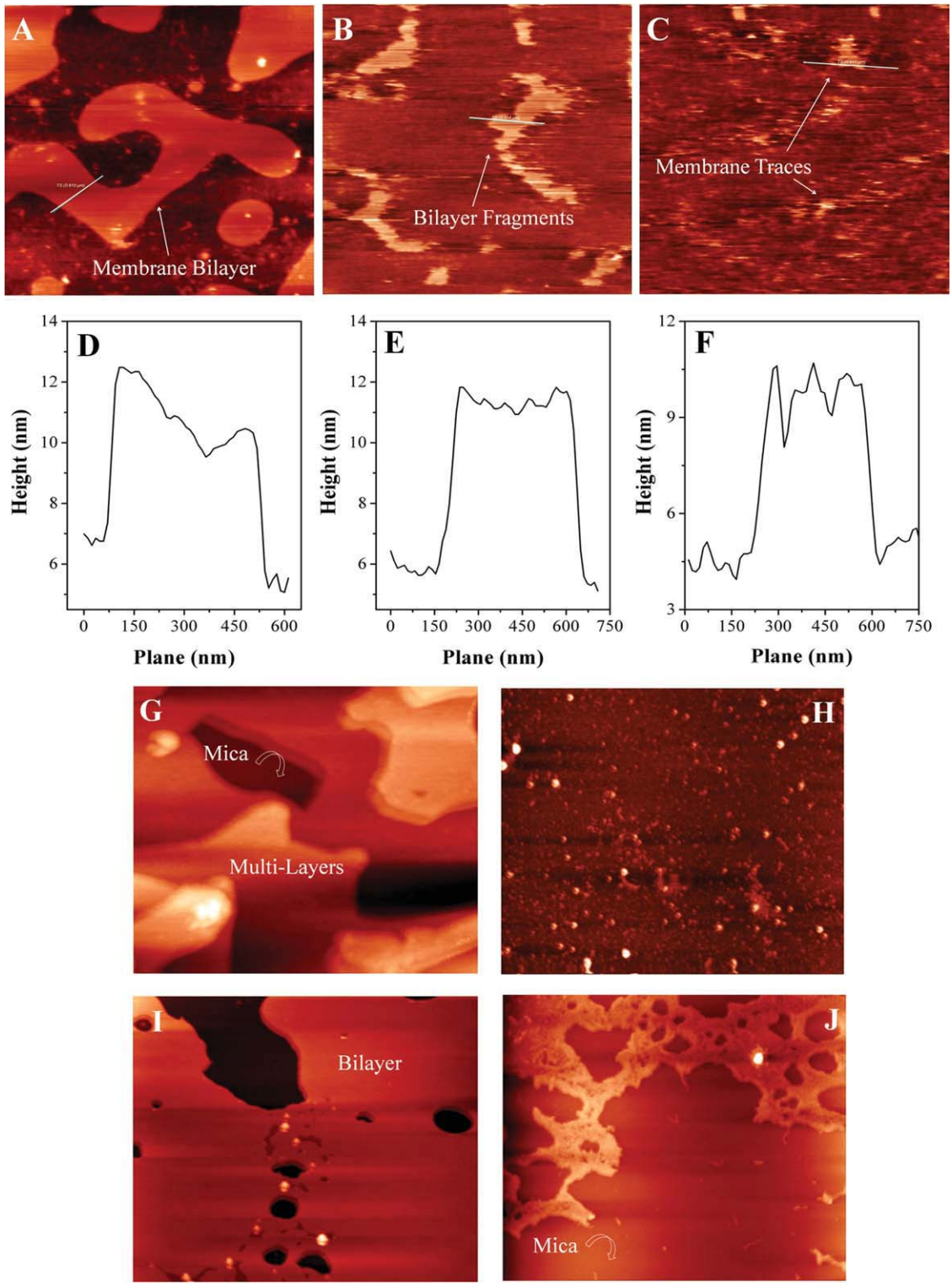

Figure 5. Atomic force microscopic studies to investigate the effect of PDC-109 on model membranes. (A) AFM image of DPPC bilayer in liquid cell (3 × 3 μm). (B) DPPC incubated with 1.5 mg/mL of PDC-109 for 10 min (3 × 3 μm). (C) DPPC incubated with same concentration of PDC-109 for a reasonably longer duration of 25-30 min (3 × 3 μm). (D, E, and F) Height profiles of the regions corresponding to the white bars marked in A, B, and C, respectively. (G) DMPC multi-layers in air (1.5 × 1.5 μm). (H) DMPC in the presence of 0.5 mg/mL of PDC-109 (5 × 5 μm). (I) DMPG bilayer in air (3.5 × 3.5 μm). (J) DMPG in the presence of 0.5 mg/mL of PDC-109 (10 × 10 μm). [Color figure can be viewed in the online issue, which is available at wileyonlinelibrary.com.]

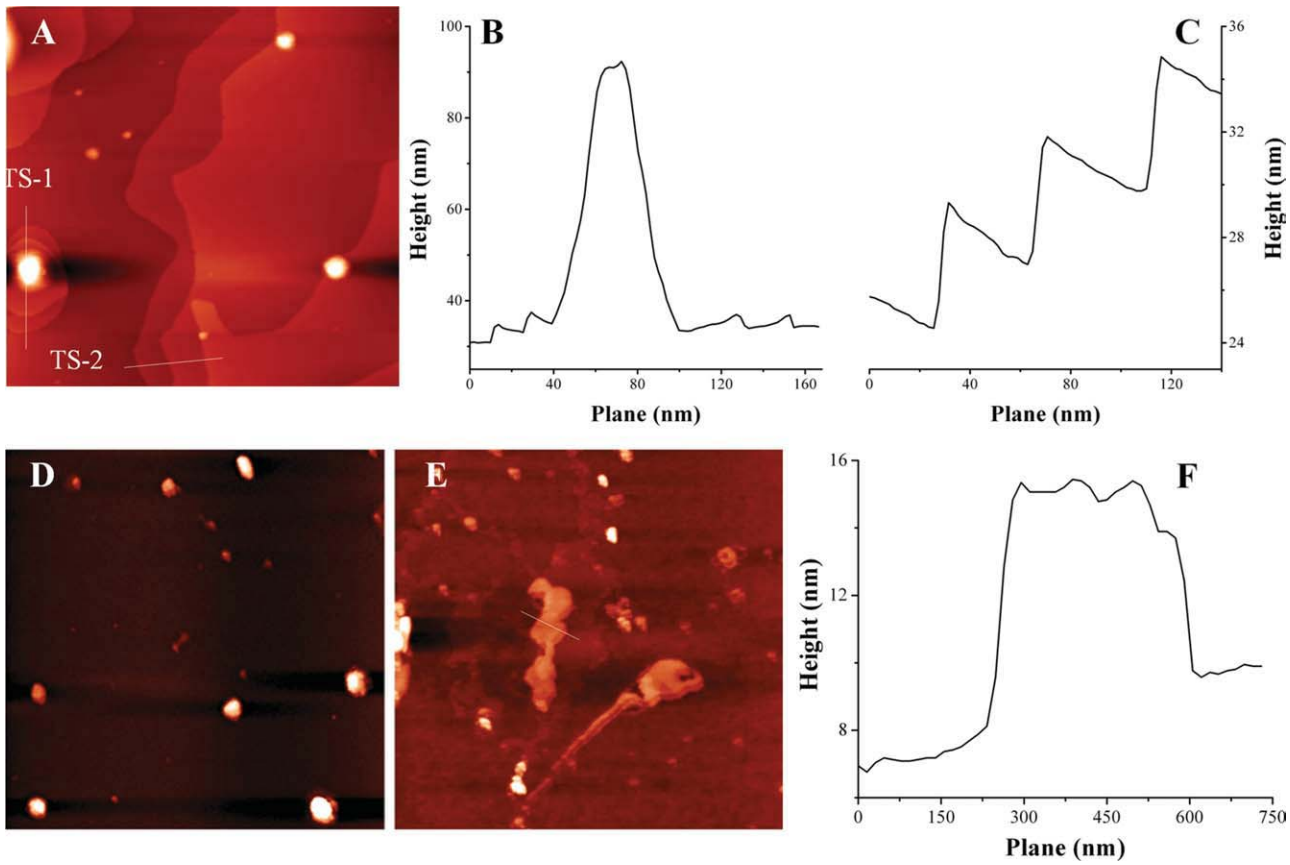

Figure 6. Cholesterol induced stabilization of DPPC model membranes. (A) AFM image of DPPC multi-layers, containing cholesterol at a ratio of 1:1 (mol/mol). Image size is 5 × 5 μm. (B) Height profile for transverse section 1 (TS1), as shown in panel A. (C) Height profile for transverse section 2 (TS2), as shown in panel A. (D) Small DPPC model membrane fragments and aggregated structures composed of PDC-109 and model membrane (5 × 5 μm). (E) Images of intact membrane fragments, observed after the action of PDC-109 on DPPC model membranes containing 40 mol% cholesterol (5 × 5 μm). (F) Height profile for transverse section, shown in panel E. [Color figure can be viewed in the online issue, which is available at wileyonlinelibrary.com.]

is consistent with the above ^{31}P NMR findings. A height profile corresponding to the region marked with a white bar in Fig. 6E is shown in Fig. 6F. The height of the membrane measured from this profile is about 5–7 nm, which is consistent with a bilayer architecture.

In summary, in this study, several lines of direct evidence are presented to demonstrate that the binding of PDC-109 to different cell membranes, model membranes (MLVs) and supported membrane layers leads to the extraction of lipids and cholesterol, which ultimately results in membrane destabilization. These results assume significance in view of the relevance of PDC-109-membrane interaction to the capacitation of spermatozoa. Presence of cholesterol provided a partial stabilization to the membrane both in gel and liquid crystalline phases. Our ^{31}P NMR studies also clearly show that binding of PDC-109 to PC and phosphatidylglycerol membranes results in the formation of micelles or SUVs and excludes the formation of inverse hexagonal and cubic phases. AFM and ^{31}P NMR studies further confirm the higher selectivity of PDC-109 toward choline phospholipids as compared with other phospholipids such as phosphatidylethanolamine and phosphatidylglycerol. Overall, these results provide direct and conclusive evidence for the earlier observations and support the model in which interaction of PDC-109 with cell plasma membranes and model membranes containing choline phospholipids results in their destabilization, leading to the formation of small lipoprotein particles [*22–24, 29, 38*]. This process is strongly dependent on the lipid composition, wherein the presence of choline phospholipids at high concentration leads to destabilization of the membrane, whereas the ability of PDC-109 to disrupt membranes containing other phospholipids, such as phosphatidylglycerol, is significantly lower, and incorporation of cholesterol affords a partial protection to the lamellar structure of the membrane [*24, 28, 29*].

ACKNOWLEDGEMENTS

This work was supported by a research grant from the Department of Science and Technology (India) to Musti J. Swamy. We thank Dr. K. Babu Rao (Lam Farm, Guntur, Sri Venkateswara Veterinary University) for kindly providing samples of bovine semen. Rajani S. Damai, Rajeshwer S. Sankhala, and V. Anbazhagan were supported by Senior Research Fellowships from CSIR (New Delhi, India). We acknowledge the University Grants Commission (India) for their support through the UPE and CAS programs, to the University of Hyderabad and School of Chemistry, respectively.

REFERENCES

1. Yanagimachi, R. (1994) Mammalian fertilization. In *The Physiology of Reproduction*, 2nd edn. (Knobil E. and Neill J. D., ed.). pp. 189–317, Raven Press, New York.
2. Chang, M. C. (1951) Fertilizing capacity of spermatozoa deposited into the fallopian tubes. *Nature* **168**, 697–698.
3. Austin, C. R. (1952) The capacitation of the mammalian sperm. *Nature* **170**, 326.
4. Harrison, R. A. P. (1996) Capacitation mechanisms and the role of capacitation as seen in eutherian mammals. *Reprod. Fertil. Dev.* **8**, 581–596.
5. Visconti, P. E., Calantino-Hormer, H., Moore, G. D., Bailey, J. L., Ning, X., Fornes, M., and Kopf, G. S. (1998) The molecular basis of sperm capacitation. *J. Androl.* **19**, 242–248.
6. Shivaji, S., Scheit, K. H., and Bhargava, P. M. (1990) *Proteins of Seminal Plasma* p. 526, Wiley, New York.
7. Manjunath, P., Sairam, M. R., and Uma, J. (1987) Purification of four gelatin-binding proteins from bovine seminal plasma by affinity chromatography. *Biosci. Rep.* **7**, 231–238.
8. Manjunath, P. and Sairam, M. R. (1987) Purification and biochemical characterization of three major acidic proteins (BSP-A1, BSP-A2 and BSP-A3) from bovine seminal plasma. *Biochem. J.* **241**, 685–692.
9. Chandonnet, L., Roberts, K. D., Chapdelaine, A., and Manjunath, P. (1990) Identification of heparin-binding proteins in bovine seminal plasma. *Mol. Reprod. Dev.* **26**, 313–318.
10. Esch, F. S., Ling, N. C., Bohlen, P., Ying, S. Y., and Guillemin, R. (1983) Primary structure of PDC-109, a major protein constituent of bovine seminal plasma. *Biochem. Biophys. Res. Commun.* **113**, 861–867.
11. Seidah, N. G., Manjunath, P., Rochemont, J., Sairam, M. R., and Cheretian, M. (1987) Complete amino acid sequence of BSP-A3 from bovine seminal plasma, Homology to PDC-109 and to the collagen-binding domain of fibronectin. *Biochem. J.* **243**, 195–203.
12. Calvete, J. J., Paloma, F. V., Sanz, L., and Romero, A. (1996) A procedure for the large-scale isolation of major bovine seminal plasma proteins. *Protein Expr. Purif.* **8**, 48–56.
13. Baker, M. E. (1985) The PDC-109 protein from bovine seminal plasma is similar to the gelatin-binding domain of bovine fibronectin and a kringle domain of human tissue-type plasminogen activator. *Biochem. Biophys. Res. Commun.* **130**, 1010–1014.
14. Swamy, M. J. (2004) Interaction of bovine seminal plasma proteins with model membranes and sperm plasma membranes. *Curr. Sci.* **87**, 203–211.
15. Gasset, M., Saiz, J. L., Sanz, L., Gentzel, M., Töpfer-Petersen, E., and Calvete, J. J. (1997) Conformational features and thermal stability of bovine seminal plasma protein PDC-109 oligomers and phosphorylcholine-bound complexes. *Eur. J. Biochem.* **250**, 735–744.
16. Wah, D. A., Fernández-Tornero, C., Sanz, L., Romero, A. and Calvete, J. J. (2002) Sperm coating mechanism from the 1.8 Å crystal structure of PDC-109-phosphorylcholine complex. *Structure* **10**, 505–514.
17. Sankhala, R. S. and Swamy, M. J. (2010) The major protein of bovine seminal plasma, PDC-109, is a molecular chaperone. *Biochemistry* **49**, 3908–3918.
18. Scheit, K. H., Kemme, M., Aumuller, G., Seitz, J., Hagendorff, G., and Zimmer, M. (1988) The major protein of bull seminal plasma: biosynthesis and biological function. *Biosci. Rep.* **8**, 589–608.
19. Calvete, J. J., Raida, M., Sanz, L., Wempe, F., Scheit, K-H., Romer, A., and Töpfer-Petersen, E. (1994) Localization and structural characterization of an oligosaccharide *O*-linked to bovine PDC-109. Quantitation of the glycoprotein in seminal plasma and on the surface of ejaculated and capacitated spermatozoa. *FEBS Lett.* **350**, 203–206.
20. Desnoyers, L. and Manjunath, P. (1992) Major proteins of bovine seminal plasma exhibit novel interactions with phospholipids. *J. Biol. Chem.* **267**, 10149–10155.
21. Thérien, I., Souberand, S., and Manjunath, P. (1997) Major proteins of bovine seminal plasma modulate sperm capacitation by high-density lipoprotein. *Biol. Reprod.* **57**, 1080–1088.
22. Thérien, I., Moreau, R., and Manjunath, P. (1998) Major proteins of bovine seminal plasma and high-density lipoprotein induce cholesterol efflux from epididymal sperm. *Biol. Reprod.* **59**, 768–776.
23. Moreau, R., Thérien, I., Lazure, C., and Manjunath, P. (1998) Type II domains of BSP-A1/-A2 proteins: binding properties, lipid efflux, and sperm capacitation potential. *Biochem. Biophys. Res. Commun.* **246**, 148–154.
24. Ramakrishnan, M., Anbazhagan, V., Pratap, T. V., Marsh, D., and Swamy, M. J. (2001) Membrane insertion and lipid-protein interactions of bovine seminal plasma protein, PDC-109 investigated by spin label electron spin resonance spectroscopy. *Biophys. J.* **81**, 2215–2225.
25. Greube, A., Müller, K., Töpfer-Petersen, E., Herrmann, A., and Müller, P. (2001) Influence of the bovine seminal plasma protein PDC-109 on the physical state of membrane. *Biochemistry* **40**, 8326–8334.
26. Swamy, M. J., Marsh, D., Anbazhagan, V., and Ramakrishnan, M. (2002) Effect of cholesterol on the interaction of seminal plasma protein, PDC-109 with phosphatidylcholine membranes. *FEBS Lett.* **528**, 230–234.
27. Müller, P., Greube, A., Töpfer-Petersen, E., and Herrmann, A. (2002) Influence of the bovine seminal plasma protein PDC-109 on cholesterol in the presence of phospholipids. *Eur. Biophys. J.* **31**, 438–447.
28. Thomas, C. J., Anbazhagan, V., Ramakrishnan, M., Sultan, N., Surolia, I., and Swamy, M. J. (2003) Mechanism of membrane binding by the bovine seminal plasma protein, PDC-109. A surface plasmon resonance study. *Biophys. J.* **84**, 3037–3044.
29. Gasset, M., Magdaleno, L., and Calvete, J. J. (2000) Biophysical study of the perturbation of model membrane structure caused by seminal plasma protein PDC-109. *Arch. Biochem. Biophys.* **374**, 241–247.
30. Anbazhagan, V., Damai, R. S., Paul, A., and Swamy, M. J. (2008) Interaction of the major protein from bovine seminal plasma, pdc-109 with phospholipid membranes and soluble ligands investigated by fluorescence approaches. *Biochim. Biophys. Acta* **1784**, 891–899.
31. Damai, R. S., Anbazhagan, V., Rao, K. B., and Swamy, M. J. (2009) Fluorescence studies on the interaction of choline-binding domain b of the major bovine seminal plasma protein, pdc-109 with phospholipid membranes. *Biochim. Biophys. Acta* **1794**, 1725–1733.
32. Anbazhagan, V. and Swamy, M. J. (2005) Thermodynamics of phosphorylcholine and lysophosphatidylcholine binding to the major protein of bovine seminal plasma, PDC-109. *FEBS Lett.* **579**, 2933–2938.
33. Laemmli, U. K. (1970) Cleavage of structural proteins during assembly of bacteriophage T4. *Nature* **227**, 680–685.

34. Harlos, K. and Eibl, H. (1980) Influence of calcium ions on phosphotidylglycerol. Two separate lamellar structures. *Biochemistry* **19**, 895–899.
35. Müller, P., Erlemann, K. R., Müller, K., Calvete, J. J., Töpfer-Petersen, E., Marienfield, K., and Herrmann, A. (1998) Biophysical characterization of the interaction of the bovine seminal plasma protein PDC-109 with phospholipid vesicles. *Eur. Biophys. J.* **27**, 33–41.
36. Grandbois, M., Clausen- Schaumann, H., and Gaub, H. (1998) Atomic force microscope imaging of phospholipid bilayer degradation by Phospholipase-A_2. *Biophys. J.* **74**, 2398–2404.
37. Milhiet, P-E., Gubellini, F., Berquand, A., Dosset, P., Rigaud, J-L., Grimellec, C. L., and Lévy, D. (2006) High-resolution AFM of membrane proteins directly incorporated at high density in planar lipid bilayer. *Biophys. J.* **91**, 3268–3275.
38. Moreau, R. and Manjunath, P. (1999) Characterization of lipid efflux particles generated by seminal phospholipid-binding proteins. *Biochim. Biophys. Acta* **1438**, 175–184.
39. Lis, L. J., McAlister, M., Fuller, N., Rand R. P., and Parsegian, V. A. (1982) Interactions between neutral phospholipid bilayer membranes. *Biophys. J.* **37**, 657–665.